Preparation of glassy carbon from lignins and lignin condensates

The preparation of carbon materials from synthetic polymers such as phenolformaldehydes, fluoropolymers, polyfurfurylalcohol, epoxides, diazopolymers, polyglutaronitrile, polyacrylonitrile and polyvinylchloride is well documented [1–4]. Usually the carbon is produced in the form of fibres but the preparation of bulky samples of glassy carbon has also aroused widespread interest because of the interesting strength, density and temperature resistance relationships of these materials.

Lignin is a biopolymer which in many respects resembles phenolformaldehyde resins. It is recovered as a by-product in the paper-manufacturing industry and is therefore available as a low-priced raw material. Lignosulfonate and alkali–lignin have been used as precursors of carbon fibres when mixed with polyvinyl alcohol, polyacrylonitrile or viscose [5].

In this work the possibility of preparing bulky glassy carbon samples from pure lignins (lignosulfonate and alkali–lignin) and from their condensation products has been studied.

The applied lignosulfonate used was Rauma Lignin Ultra, sodium lignosulfonate obtained from Rauma-Repola Oy. Alkali–lignin was obtained as waste-liquour from Keskuslaboratorio Oy. The lignin was separated from waste-liquour by $CHCl_3$-H_2SO_4 treatment [6]. Lignosulfonate was condensed with H_2O_2 [7], with NaOH + HCl [8] and with phenol–formaldehyde (*PF*) [9]. Alkali–lignin was condensed with formaldehyde (*F*) [10] and with phenol–formaldehyde [9].

The lignins and their condensates were dried and ground by hand until of particle-size less than 250 μm. These powders were pressed to cylindrical samples (of diameter 13 mm and height typically 3 mm). The compression pressure of 10 MPa was applied for 2 min. The samples were pyrolyzed in a nitrogen atmosphere using the 26 h pyrolyzing programme developed earlier [4]: the temperature of lignin samples was first raised rapidly to 180° C and thereafter the temperature was increased by 18.5° C h^{-1} to 750° C and then raised rapidly to 1000° C, the cooling of the furnace was carried out in about an hour.

The properties of end-products were studied measuring bulk densities, apparent porosities (by the method ASTM C 373-72) and compressive strengths of between 3 and 5 apparently identical samples. Mechanical tests were carried out using an Instron 1115 TT-DM-L machine using test speeds of 2 to 3 mm min^{-1} at a temperature of 23° C. The microstructures of the fracture surfaces of samples were studied by a JEOL JSM-U3 scanning electron microscope.

The experimental results are given in Table I. Both compressed lignosulfonates and alkali–lignins give comparatively good yields of carbon with satisfactory compressive strengths. The condensation reactions increase the carbon yield in the case of alkali–lignin. In the case of the lignosulfonate the increase of carbon yield is not significant. Bulk densities of lignosulfonate carbons (excluding H_2O_2-condensate) are higher and apparent porosities lower than the corresponding values of alkali–lignin condensates. This seems to be a consequence of the high ash content of lignosulfonate (10.3 wt %). This could be observed

TABLE I Properties of glassy carbons prepared from lignins and lignin condensates

Sample	Yield (%)	Apparent porosity (%)	Bulk density (g cm^{-3})	Compressive strength (N mm^{-2})
Lignosulfonate				
Non-condensed	45 ± 0.5	36 ± 2	1.20	95 ± 25
H_2O_2-condensate	43 ± 2	40 ± 1	1.14	70 ± 10
NaOH + HCl-condensate	47 ± 2	33 ± 1	1.34	90 ± 40
PF-condensate	45 ± 1	38 ± 2	1.16	75 ± 15
Alkali–lignin				
Non-condensed	42 ± 2	40 ± 1	1.15	110 ± 30
F-condensate	47 ± 2	38 ± 2	1.16	110 ± 20
PF-condensate	45 ± 1	38 ± 1	1.17	100 ± 25

0022–2461/81/010272–03$02.30/0

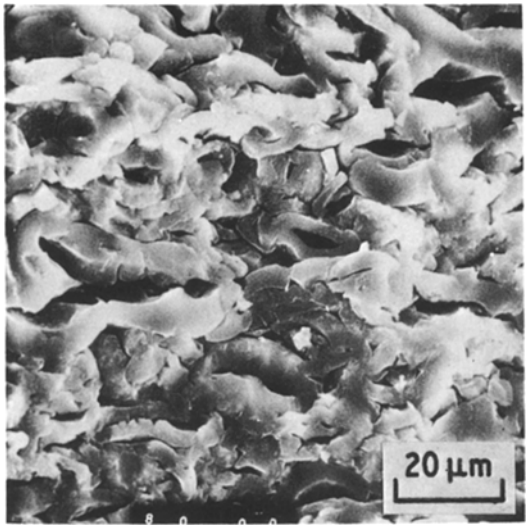

Figure 1 Scanning electron micrograph of the microstructure of lignosulfonate carbon.

also macroscopically because sodium oxide formed white layers on the surfaces of several lignosulfonate carbon samples. In air these layers reacted rapidly with the moisture producing sodium hydroxide. Despite their higher bulk densities and lower apparent porosities, the compressive strengths of lignosulfonate carbon samples were lower than those of alkali–lignin carbon samples. This is also evidence of the deteriorating effect of high ash content upon the structure of lignosulfonate carbon. Alkali–lignin carbon samples macroscopically resembled glassy carbon which can be prepared from *PF*-resins [1, 4].

The internal structure of lignosulfonate carbon comprised sphere-like partially sintered granules which were often hollow (Fig. 1). The granules were also flattened in the vertical compression direction.

The internal structure of lignosulfonate condensate carbons did not show any more globular aggregates (Fig. 2).

Alkali–lignin carbon showed a more regular structure where pores were more globular and fusion of lignin powder particles was more complete than was seen for lignosulfonate carbons (Fig. 3).

On the basis of the above experiments it was concluded that unmodified alkali–lignin is a suitable raw material for production of glassy carbon. Evidently the optimization of compression and pyrolysis conditions would give carbons with still better properties. For example, it was shown that when the carbonization temperature was increased at a rate of only $6^\circ C h^{-1}$ (instead of $18.5^\circ C h^{-1}$) 41% of alkali–lignin carbon with the compressive strength of $155 \pm 10 N mm^{-2}$ was obtained. This value is about half the compressive strength of *PF*-resin based glassy carbons [1, 4], which already have many practical applications [1].

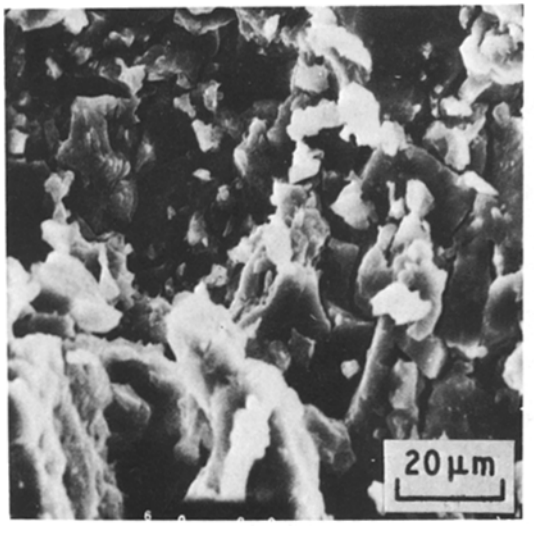

Figure 2 Scanning electron micrograph of the microstructure of lignosulfonate H_2O_2-condensate carbon.

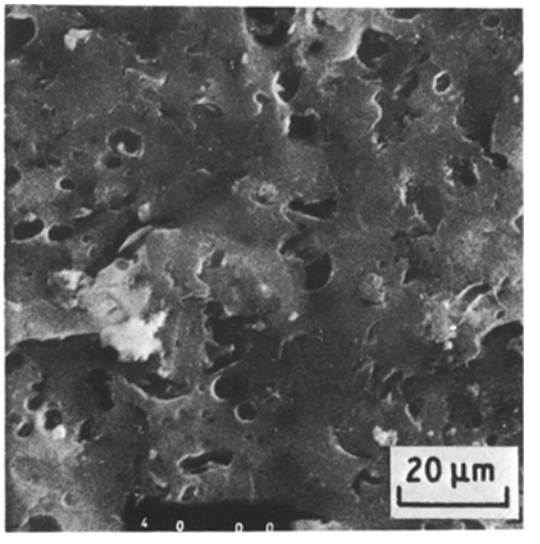

Figure 3 Scanning electron micrograph of the microstructure of alkali–lignin carbon.

References

1. G. M. JENKINS and K. KAWAMURA, "Polymeric Carbons – Carbon Fibre, Glass and Char" (Cambridge University Press, Cambridge, 1976).
2. P. L. WALKER, ed., "Chemistry and Physics of Carbon" (Marcel Dekker, New York, 1971).
3. B. LÖFGREN, J. RAUTAVUORI and P. TÖRMÄLÄ, *Acta Chem. Scand.* **A31** (1977) 703.
4. J. RAUTAVUORI and P. TÖRMÄLÄ, *J. Mater. Sci.* **14** (1979) 2020.
5. S. OTANI, K. FUKUOKA, Y. FUKUOKA, B. IGARASHI and K. SASAKI, U.S. Patent Number 3 461 082 (1969).
6. D. M. WHALEN, *Tappi* **58** (1975) 110.
7. H. H. NIMZ, I. MOHARAB and I. GURANG, *Appl. Polymer Symp.* **28** (1976) 1225.
8. O. SÜSSENGUTH and G. ZIENERT, F. R. Germany Patent Number 921 776 (1954).
9. W. R. MOFFITT and B. B. MORRIS, U.S. Patent Number 3 227 667 (1967).
10. J. MARTON, T. MARTON and S. I. FALKEHAG, *Adv. Chem. Ser.* **59** (1966) 125.

Received 14 April
and accepted 12 May 1980.

PERTTI TÖRMÄLÄ
MATTI ROMPPANEN
Institute of Materials Science,
Tampere University of Technology,
P.O.B. 527, SF-33101 Tampere 10,
Finland

Some characteristics of the ferrite $Ba_3Fe(II)_4Fe(III)_{28}O_{49}$

It is well known that oxides of the form $2BaO–11Fe_2O_3$ are used for the fabrication of permanent magnets because they exhibit better magnetic characteristics than the hexaferrite $BaO–6Fe_2O_3$. According to Brady [1], these materials are made of a mixture of the hexaferrite $BaFe_{12}O_{19}$ (with specific saturation magnetization, σ_S, equal to 72.0 emu g^{-1} at room temperature) and of the ferrite $Ba_3Fe(II)_4Fe(III)_{28}O_{49}$ (σ_S = 79.6 emu g^{-1} at room temperature). This oxide, containing divalent iron, crystallizes as the hexaferrite with a magnetoplumbite structure and, it is suggested, corresponds to the structural model MYS_N or $MT(S_N)_2$ ($Y = TS_N$) such that

$$M \equiv BaFe(III)_{12}O_{19} ;$$

$$T \equiv Ba_2Fe(III)_8O_{14} ;$$

$$(S_N)_2 \equiv 2(Fe(II)_2Fe(III)_4O_8) ,$$

and so

$$MYS_N \equiv Ba_3Fe(II)_4Fe(III)_{28}O_{49} .$$

It is noticeable that the specific saturation magnetization calculated for such a model (σ_S = 67.4 emu g^{-1}), assuming that it corresponds to the addition of the magnetization of each block, is lower than the value reported by Brady [1] for the specific saturation magnetization measured at room temperature (σ_S = 79.6 emu g^{-1}). Therefore the ferrite $Ba_3Fe(II)_4Fe(II)_{28}O_{49}$ was prepared and a measurement of its specific saturation magnetization was made.

A study of the reactivity of potassium ferrites $K_2O–nFe_2O_3$ with a molten barium salt led an investigation of the different metastable barium ferrites $BaO–nFe_2O_3$. Among them, the ferrite $3BaO–16Fe_2O_3$ ($Ba_3Fe(III)_{32}O_{51}$) presents the same ratio Fe/Ba = 32/3 as the oxide reported by Brady. The important characteristics of this new oxide, which have been described elsewhere [2], are that its X-ray diffraction pattern is very similar to that of the hexaferrite $BaFe(III)_{12}O_{19}$ and that its chemical composition and its specific saturation magnetization (σ_S = 88.1 emu g^{-1} at 4 K) agree with a type M_6Y' or M_6TS_L ($Y' = TS_L$) structural model such that

$$6M \equiv 6(BaFe(III)_{12}O_{19});$$

$$T \equiv Ba_2Fe(III)_8O_{14} ;$$

$$3S_L \equiv Fe(III)_{16}O_{24}$$

so that

$$3M_6Y' \equiv 8Ba_3Fe(III)_{32}O_{51} ,$$

in which S_L corresponds to an element with a vacancy spinel structure, $Fe(III)_6$ $[Fe(III)_{10}$ $\square_2]O_{24}$, where $\square$ represents a vacancy, similar to those of the oxide γFe_2O_3. The specific saturation magnetization calculated for this model is σ_S = 88.0 emu g^{-1}.

0022–2461/81/010274–02$02.20/0